Correspondence

High-Frame-Rate Echocardiography With Reduced Sidelobe Level

Hideyuki Hasegawa and Hiroshi Kanai

***Abstract*—Echocardiography has become an indispensable modality for diagnosis of the heart. It enables observation of the shape of the heart and estimation of global heart function based on B-mode and M-mode imaging. Methods for echocardiographic estimation of myocardial strain and strain rate have also been developed to evaluate regional heart function. Furthermore, it has been recently shown that echocardiographic measurements of transmural transition of myocardial contraction/relaxation and propagation of vibration caused by closure of the heart valve would be useful for evaluation of myocardial function and viscoelasticity. However, such measurements require a frame rate (typically >200 Hz) much higher than that achieved by conventional ultrasonic diagnostic equipment. We have recently realized a high frame rate of about 300 Hz with a full field of view of 90° using diverging transmit beams and parallel receive beamforming. Although high-frame-rate imaging was made possible by this method, the side lobe level was slightly larger than that of the conventional method. To reduce the side lobe level, phase coherence imaging has recently been developed. Using this method, the spatial resolution is improved and the side lobe level is also reduced. However, speckle-like echoes, for example, echoes from the inside of the heart wall, are also suppressed. In the present study, a method for reducing the side lobe level while preserving speckle-like echoes was developed. The side lobe level was evaluated using a wire phantom. The side lobe level of the high-frame-rate imaging using unfocused diverging beams was improved by 13.3 dB by the proposed method. In *in vivo* measurements, a B-mode image of the heart of a 23-year-old healthy male could be obtained while preserving the speckle pattern in the heart wall at a frame rate of 316 Hz with a full field of view of 90°.**

I. Introduction

Echocardiography is a predominant modality for diagnosis of the heart because it provides a cross-sectional image of the heart noninvasively in real time. Because of the high temporal resolution of ultrasonic diagnostic equipment, global heart function, such as ejection fraction (EF), can be estimated based on B-mode and M-mode imaging much more easily than with other diagnostic modalities, such as magnetic resonance imaging (MRI) and computed tomography (CT). It has recently been shown that ultrasonic measurements of transmural transition of myocardial contraction/relaxation and its propagation [1], [2] and propagation of vibration caused by closure of a heart valve would be useful for evaluation of myocardial function and viscoelasticity [3], [4]. However, such measurements require a frame rate much higher than that achieved by conventional ultrasonic diagnostic equipment. For example, electrical excitation propagates in Purkinje fibers and ventricular muscle at typical velocities of 0.3 to 4 m/s [5], and the corresponding propagation velocities of myocardial contraction of 0.5 to 7 m/s have been measured by ultrasound [4], [6]. In these studies, a high frame rate (typically higher than 400 Hz with a slightly reduced lateral field of view, which is much higher than that realized by conventional ultrasonic diagnostic equipment, usually several tens of hertz) is required to measure the propagation of this electromechanical wave and the resulting transient small motion of the heart wall.

Konofagou *et al.* [7] and D'hooge *et al.* [8] increased the frame rate to above 200 Hz in the ultrasonic measurement of the heart function. However, the size of the field of view and the total number of scan lines in an ultrasonic image were significantly reduced.

To achieve a high frame rate, we used sparse sector scanning, in which the number of scan lines was decreased to about 10 [9], and applied it to various applications [1]–[4]. In this method, the angle intervals between scan lines are increased to obtain a large lateral field of view with a small number of scan lines. Therefore, the lateral image resolution is significantly degraded.

The aforementioned methods are based on conventional beamforming; therefore, the density of scan lines or field of view must be sacrificed to achieve a high frame rate. To overcome this problem, parallel receive beamforming [10] with a wide transmit beam has been developed to illuminate a wider region by one transmission to reduce the number of transmissions. Lu and colleagues proposed an imaging method using an unfocused but nondiverging transmit beam, namely, a limited diffraction beam [11]–[14]. Unfocused beams achieved a wider beam width, and nondiverging beams used in these cited studies prevented the insonified energy from being spread to ensure that the required penetration depth was achieved. However, the width of a nondiverging beam is limited by the size of the aperture, which would limit the number of receiving beams created by one transmission.

High-frame-rate echocardiography at about 300 Hz with a full field of view of 90° using steered diverging transmit beams and parallel receive beamforming has recently been realized [15]. Diverging waves were produced using all transducer elements in an ultrasonic array probe to obtain ultrasonic echoes with a better SNR [16], [17] than the spherical wave produced by a single element [18]. Although just the idea of a diverging beam produced from multiple elements was shown in [17], the feasibility of the diverging beam had not been examined. The diverging beam from multiple elements was shown to be feasible in high-frame-rate echocardiography [15]. Although high-frame-rate imaging is possible by our method, the side lobe

Manuscript received December 20, 2011; accepted July 20, 2012.

The authors are with the Graduate School of Biomedical Engineering and the Graduate School of Engineering, Tohoku University, Sendai, Japan (e-mail: hasegawa@ecei.tohoku.ac.jp).

DOI http://dx.doi.org/10.1109/TUFFC.2012.2490

level is slightly larger than that of conventional beamforming. To reduce the side lobe level, phase coherence imaging has recently been developed [19]. This method sensitively suppresses echoes influenced by the diversity of phases of echoes received by transducer elements because of various factors, such as focusing error, etc. Therefore, the spatial resolution is improved and the side lobe level is suppressed by this method, but weak speckle-like echoes, which are generated by interference of scattered echoes, are also significantly suppressed because the phases of echoes would be influenced by the interference. In the present study, a method to reduce the side lobe level while preserving speckle-like echoes was developed. The side lobe level was evaluated using a wire phantom, and a B-mode image of a heart of a 23-year-old healthy male was obtained *in vivo* by the proposed method.

II. Principles

Using an unfocused wide transmit beam increases the side lobe level compared with conventional beamforming (focusing both in transmit and receive). Therefore, methods for reduction of the side lobe level are required.

When receive focusing is performed with respect to a spatial point $\mathbf{p}$, the position of the source of an echo does not always exactly coincide with $\mathbf{p}$. Let us consider the difference between the time delay applied by a receive beamformer and the propagation time delay of the echo. As shown in Fig. 1(a), the locations of focus and the source of the echo are defined by (x, z) and $(x + \Delta x, z + \Delta z)$, respectively. Under such conditions, distance r_i' from the ith element to the source and distance r_i from the ith element to the focal point are expressed as

$$r_i' = \sqrt{(x - x_i + \Delta x)^2 + (z + \Delta z)^2}, \tag{1}$$

$$r_i = \sqrt{(x - x_i)^2 + z^2}, \tag{2}$$

where x_i is the lateral position of the ith element.

Residual time delay $\Delta\tau_i$ (focusing error) of the echo from the source received by the ith element after receive beamforming (applying time delay $T_{\mathrm{RBF},i}$) depends on the difference between r_i and r_i'.

$$\begin{aligned}(r_i')^2 - r_i^2 &= \Delta r_i(2r_i + \Delta r_i) \\ &= (x - x_i + \Delta x)^2 + (z + \Delta z)^2 - (x - x_i)^2 - z^2,\end{aligned} \tag{3}$$

where Δr_i is $r_i' - r_i$.

By assuming that the focal depth z is sufficiently large, squares of Δx and Δz can be neglected:

$$\Delta r_i(2r_i + \Delta r_i) \approx 2\Delta x(x - x_i) + 2\Delta z \cdot z, \tag{4}$$

$$\begin{aligned}\Delta r_i &= \frac{2\Delta x(x - x_i) + 2\Delta z \cdot z}{2r_i + \Delta r_i} \\ &\approx \frac{\Delta x(x - x_i) + \Delta z \cdot z}{r_i},\end{aligned} \tag{5}$$

where $2r_i + \Delta r_i$ is approximated by $2r_i$ because Δr_i is assumed to be sufficiently smaller than $2r_i$.

For large z, distance r_i can be approximated to be $(x^2 + z^2)^{1/2}$ because x_i is limited by the aperture size (x_i was less than 10 mm in the present study). Therefore, residual time delay $\Delta\tau_i$ is expressed as

$$\begin{aligned}\Delta\tau_i &= \frac{\Delta r_i}{c_0} \\ &\approx ax_i + b,\end{aligned} \tag{6}$$

where c_0 is the speed of sound. Constants a and b are given by

$$a = \frac{\Delta x}{c_0\sqrt{x^2 + z^2}}, \tag{7}$$

$$b = \frac{\Delta x \cdot x + \Delta z \cdot z}{c_0\sqrt{x^2 + z^2}}. \tag{8}$$

Residual time delay $\Delta\tau_i$ is also expressed as the residual phase delay $\Delta\theta_i$:

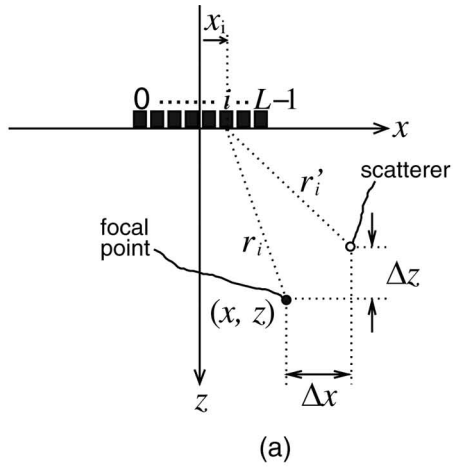

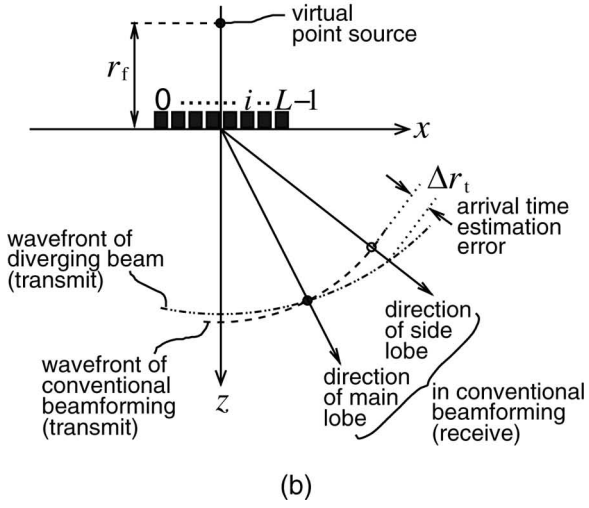

Fig. 1. Illustration of mismatch between the location of a focal point and that of the source of an echo (a) in receive and (b) in transmission.

$$\Delta\theta_i = 2\pi f_0 \Delta\tau_i, \tag{9}$$

where f_0 is the center frequency of ultrasound. In the present study, a method was proposed for reduction of the side lobe level while keeping the shape of the point spread function similar to those in conventional beamforming and our proposed method using diverging beams. As shown in (6), there is a linear relationship between the residual phase delay $\Delta\theta_i$ and the lateral position x_i of an element when the location of a focal point is close to that of a scatterer. This means that the difference between residual phase delays of two neighboring elements is consistent across the array when the focusing is done near the source of an echo (when Δx and Δz are small). This consistency can be evaluated by the magnitude-squared coherence function (MSCF) γ [20], defined as:

$$\gamma = \frac{\left|\sum_{i=0}^{L-2} S_i^* \cdot S_{i+1}\right|^2}{\sum_{i=0}^{L-2} |S_i|^2 \sum_{i=0}^{L-2} |S_{i+1}|^2}, \tag{10}$$

where L is the number of elements. The numerator in (10) corresponds to the cross-spectrum between S_i and S_{i+1} averaged across the array. Therefore, the MSCF becomes 1 when the transfer function from S_i to S_{i+1} is constant across the array. On the other hand, the magnitude of the numerator decreases because of the incoherent averaging of the transfer function when the transfer function is not constant. The phase of the transfer function corresponds to the phase difference between two neighboring elements. Therefore, the MSCF would decrease when the phase difference between two neighboring elements is not constant [= nonlinear according to the element number (position)].

To obtain the MSCF γ, the complex Fourier coefficient S'_i at f_0 (= 3.75 MHz) of the RF echo signal $s_i(t - T_{\mathrm{RBF},i})$ received by the ith transducer element must be estimated. To obtain the complex Fourier coefficient S'_i, in the present study, the discrete Fourier transform at f_0 was applied to $s_i(t - T_{\mathrm{RBF},i})$ with a Hann window whose length was 0.53 μs. Under this condition, the first nulls of the power spectrum of the Hann window were located at 0 and 7.5 MHz, providing the available maximum bandwidth of the resultant complex signal S_i sampled at 30 MHz.

The Fourier transform was applied to the RF echo $s_i(t - T_{\mathrm{RBF},i})$ received by the ith transducer element after the time shift by the receiving beamformer to account for the differences among propagation time delays of echoes received by transducer elements. However, the time delay $T_{\mathrm{RBF},i}$ is an integral multiple of the sampling interval of the RF echo. To remove the residual time delay resulting from the difference between the actual time delay $\Delta\tau_i$ and $T_{\mathrm{RBF},i}$, S'_i is multiplied by $\exp\{2\pi f_0(\Delta\tau_i - T_{\mathrm{RBF},i})\}$ to obtain the corrected Fourier coefficient S_i in (10). Therefore, there are no phase differences among corrected Fourier coefficients $\{S_i\}$ when the location of the source of the echo exactly coincides with the focal point $\mathbf{p}$ [the relationship between residual time delay and an element's lateral position is linear, but both a and b in (6) are zero]. In this case, the MSCF γ is 1. In addition, according to (6) and (9), there is a linear relationship between the phase delay $\Delta\theta_i = \angle S_i$ and the lateral position x_i of the transducer element when the focal point is located very near the source of the echoes (small Δx and Δz). In such cases, the MSCF γ is also close to 1 because the phase difference between the spectra of the signals received by ith and $(i+1)$th elements is consistent across the array. On the other hand, the MSCF γ decreases when there is a mismatch between the locations of the source of an echo and the focal point, (e.g., echoes caused by side lobes) because the assumption of (4) is not applicable. Therefore, such undesirable echoes can be suppressed by weighting the beamformed RF signal at $\mathbf{p}$ using the MSCF γ.

Furthermore, the difference between transmit beams in conventional and proposed beamforming is considered to affect the side lobe reduction. In conventional beamforming, the geometrical center (center of the aperture) is same in both transmit and receive, as illustrated in Fig. 1(b). Therefore, the time required for the propagation of ultrasound from the aperture to a scatterer (in transmit) and that from the scatterer to the aperture (in receive) are same, and an echo from a scatterer, which is located at the range distance along the side lobe that is same as the range distance of the focal point, would contribute to the calculation of the MSCF at the spatial point $\mathbf{p} = (x, z)$.

On the other hand, the time required for the propagation from the aperture to the scatterer and that from the scatterer to the aperture are different in our beamforming using diverging beams because the geometrical center of the transmit beam is the position of a virtual source of a diverging beam. The time required for the propagation of a diverging beam from the aperture to a scatterer can be estimated correctly when the scatterer is located at the focal point. However, there is an arrival-time estimation error Δr_{t}, which reduces the contribution of the echo from the scatterer to the calculation of the MSCF at the spatial point $\mathbf{p}$ (there is no echo signal in beamforming at $\mathbf{p}$ when Δr_{t} is larger than the pulse duration of ultrasound) when the scatterer is not at the focal point. Such arrival-time estimation error would also reduce the coherence of the received signals.

III. Evaluation of Spatial Resolution and Side Lobe Level Using a Wire Phantom

In the present study, a commercial diagnostic ultrasonic system (α-10, Aloka, Tokyo, Japan) was used with a 3.75-MHz phased array probe. The phased array was composed of $L = 96$ elements at intervals of 0.2 mm. The elevation focal distance was fixed to be 70 mm. This system was modified so that all of the 96 elements can be excited simultaneously and RF echoes received by $L = 96$ individual elements could be acquired at a sampling frequency of 30 MHz and a 16-bit resolution for off-line processing (receive beamforming, compounding, etc.). In conventional beamforming, receive focusing was done with

respect to each discrete spatial point. The beamforming procedure in our high-frame-rate imaging is described in [15]. The Hann apodization was used for both conventional beamforming and our high-frame-rate imaging. In the beamforming procedure, a constant speed of sound of 1540 m/s was assumed.

In the basic experiment, fine nylon wires (diameter ≈100 μm) placed in water were used for evaluation of the spatial resolution. Figs. 2(a)–2(d) show B-mode images of the wires obtained by conventional beamforming and parallel beamforming with diverging beams at r_f = 100 mm without weighting, with weighting by the MSCF, and with weighting by the phase coherence factor [19], respectively, where r_f is the distance between the front surface of the array and the virtual point source behind the array for producing a diverging beam. The dynamic ranges of Figs. 2(a)–2(d) are 60 dB. For diverging beams, distance r_f was set at 100 mm. In Fig. 2, there is not much difference between the B-mode image obtained by conventional beamforming [Fig. 2(a)] and those obtained using diverging beams with [Fig. 2(b)] and without [Fig. 2(c)] weighting by the MSCF. The B-mode image obtained using diverging beams with weighting by the phase coherence factor [Fig. 2(d)] shows a significantly improved spatial resolution compared with the other images. In Fig. 2(d), the phase coherence factor is obtained as max[0,1 − σ/σ_0] [19], where σ is the standard deviation of phases of echoes received by individual elements and $\sigma_0 = \pi/3^{0.5}$. The standard deviation σ was evaluated after applying time delays by the receiving beamformer.

Fig. 3 shows the lateral profiles of the images [corresponding to point spread functions (PSF)] at the shallowest wire. The half-full-widths at half-maxima of the point spread functions shown in Fig. 3 are provided in Table I. From the data shown in Fig. 3, the average side lobe levels were evaluated in the lateral angular ranges, $-45° <$ (lateral angle) $< -15°$ and $15° <$ (lateral angle) $< 45°$. The side lobe level obtained using diverging beams increased by 8.5 dB compared with conventional beamforming. By weighting with the MSCF, the side lobe level in the high-frame-rate imaging using diverging beams was reduced by 13.3 dB. Weighting by the phase coherence factor showed the best spatial resolution and the lowest side lobe level in the phantom experiment.

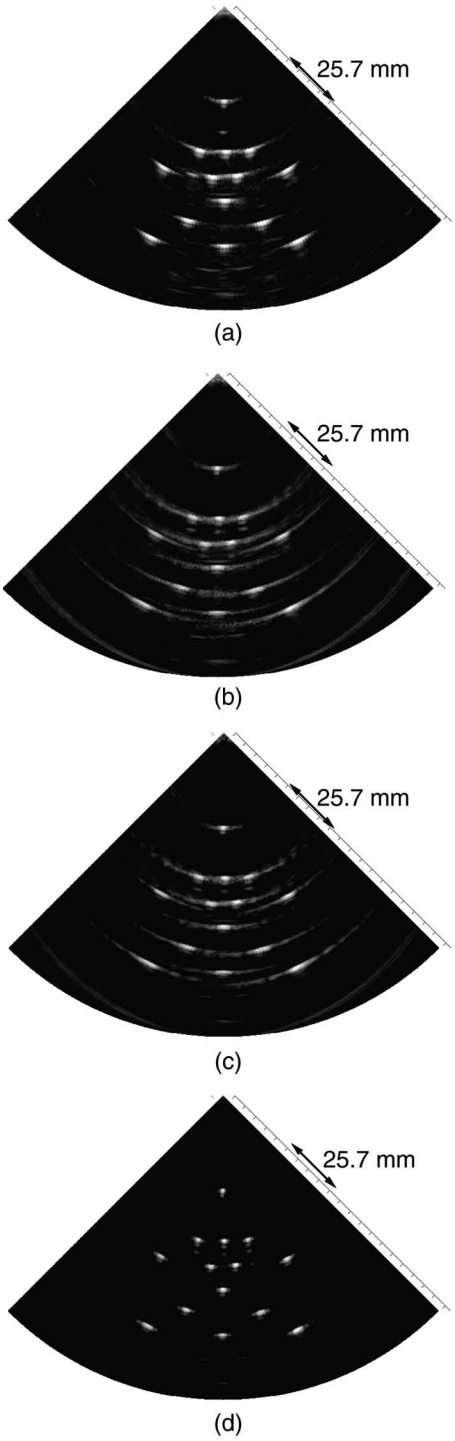

Fig. 2. B-mode images of fine wires obtained (a) by conventional sector scanning, (b) using a diverging beam, (c) using a diverging beam with weighting by the magnitude-squared coherence function (MSCF), and (d) using a diverging beam with phase coherence factor weighting [19].

IV. *In Vivo* Imaging of a Human Heart

Figs. 4(a)–4(d) show B-mode images of the heart of a 23-year-old healthy male obtained by conventional beamforming and parallel beamforming with diverging waves at r_f = 100 without weighting, with weighting by the MSCF, and with weighting by the phase coherence factor, respectively. Fig. 5 shows the intensity profiles along the scan lines indicated by the white lines in Fig. 4. Note that the position of the posterior wall in the measurement with conventional beamforming was slightly shallower than that in the measurement with diverging beams. Using diverging waves [Fig. 4(b)], a B-mode image of the heart could be obtained at a high frame rate of 316 Hz with a full lateral field of view of 90°. By weighting with the MSCF [Fig. 4(c)], the image contrast was improved, and speckle-like echoes, for example, echoes in the heart wall, were well preserved. It can be also observed in Fig. 5 that the proposed method using the MSCF suppresses the undesirable echoes in the cardiac lumen while keep-

TABLE I. HALF-FULL-WIDTHS AT HALF-MAXIMA OF POINT SPREAD FUNCTIONS SHOWN IN FIG. 3.

	Conventional beamforming	Diverging	Diverging with MSCF	Diverging phase coherence
Width of lateral PSF [mm]	0.66	0.82	0.81	0.43

ing the echoes inside the heart walls. On the other hand, by weighting with the phase coherence factor [Fig. 4(d)], speckle-like echoes inside the heart walls were significantly suppressed, although echoes resulting from specular reflection, such as an echo from the epicardium, were significantly enhanced. As shown in Fig. 3, although the spatial resolution is significantly improved by weighting with the phase coherence factor, this characteristic, i.e., significant suppression of speckle-like echoes, may not be preferable for analyzing the heart wall, such as estimation of velocity and strain rate of the heart wall.

V. DISCUSSION

Recently, we have developed a method based on parallel beamforming with diverging transmit beams for high-frame-rate echocardiography. To realize B-mode imaging in a sector format based on parallel beamforming, spherically diverging waves were used in transmission. However, in this method, the side lobe level slightly increased compared with that of conventional beamforming because of the use of unfocused transmit beams. In the present study, a method for reduction of side lobe level was developed to realize a side lobe level lower than that of conventional beamforming with a frame rate of over 300 Hz, which is much higher than that of conventional beamforming.

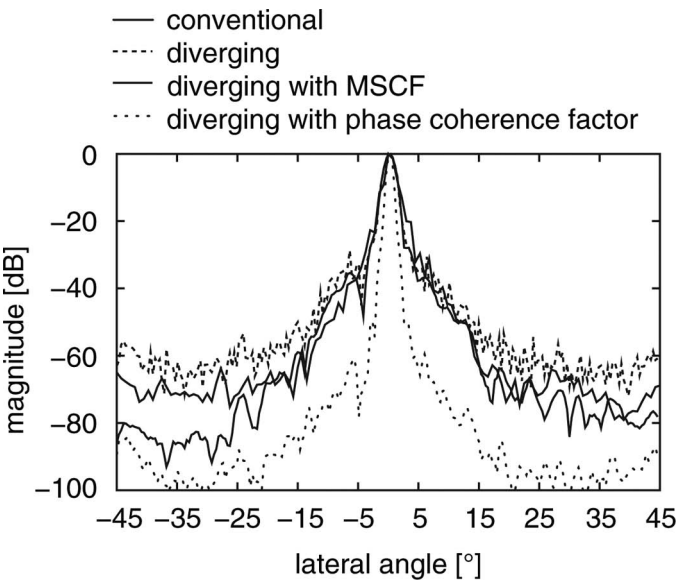

Fig. 3. Point spread functions in the lateral direction obtained by conventional sector scanning, diverging beam, diverging beam with weighting by the magnitude-squared coherence function (MSCF), and diverging beam with phase coherence factor weighting [19].

To consider small residual time delays of echoes, the phases of the echoes were used in the present study. To obtain the phase information, the Hilbert transform is used in general. However, the Hilbert transform requires the Fourier transform of the echo signal and the inverse Fourier transform of the estimated frequency spectrum. To increase the computational efficiency, in the present study, the Fourier coefficient of the echo at only the center frequency of ultrasound was calculated. This center frequency should be the center frequency of the received RF echo. However, in the present study, the center frequency of the ultrasound emitted was used because the estimation of the center frequency of the received echo required an additional computation. Before calculating the MSCF, time delays based on conventional focusing were applied to signals received by individual elements. In this procedure, sub-sample time delays were applied by considering the phase of the echo signal, as described in Section II. As expressed in (9), the phase delay coinciding with the corresponding time delay is expressed using the center frequency of the received echo. Therefore, there would be errors in application of time delays. However, such errors are negligible because the errors are smaller than the sampling interval of 25 ns.

In the results of imaging of wires, it was found that the side lobe reduction by the proposed method was depth-dependent, i.e., the side lobe reduction is smaller in a deeper region than a shallower region, because the change in the distance from a scatterer to an element caused by the lateral position of the element is smaller in a deeper region. As suggested for the phase coherence factor [19], the side lobe reduction can be controlled by taking γ^{α} (γ: MSCF), where α is a variable coefficient. Therefore, in our future work, it may be effective to control the weights by considering the depth-dependent characteristic of the MSCF γ.

To suppress the side lobe level, the phase coherence factor [19] was recently introduced. This method suppresses a beamformed echo signal whose standard deviation of phases of echoes received by transducer elements is large. Using this method, weak speckle-like echoes are also suppressed because the standard deviation of phases of echoes received by individual elements would be increased by interference of echoes, which is the source of speckle-like echoes. In some cases, it is important to observe speckle patterns of tissues. Therefore, a method for reduction of the side lobe level with preservation of speckle-like echoes was developed in the present study. On the other hand, the phase coherence factor improves spatial resolution and

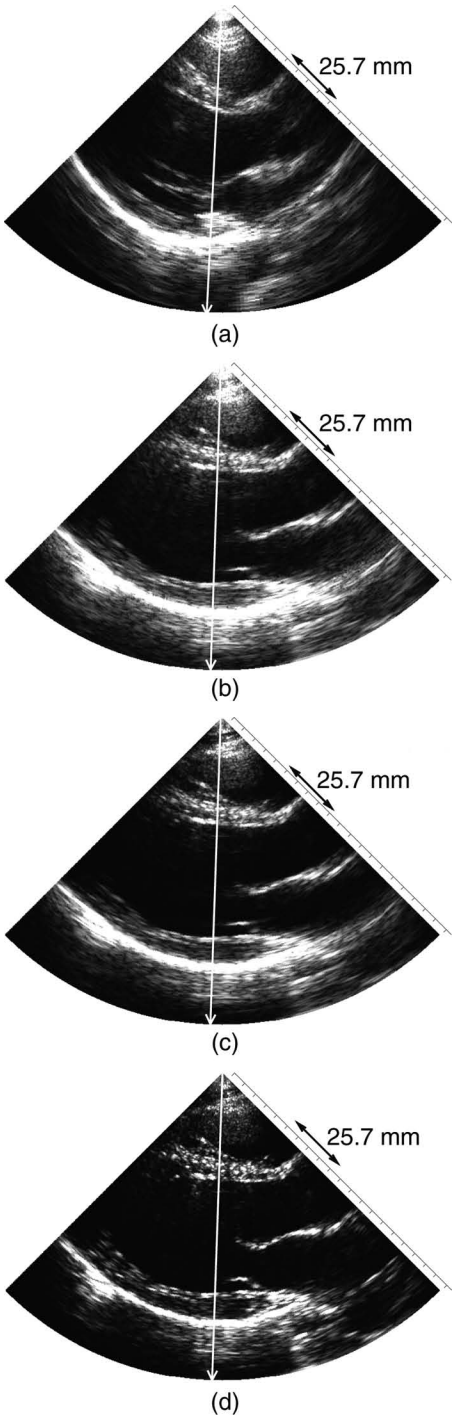

Fig. 4. B-mode images of the heart of a 23-year-old healthy male obtained (a) by conventional sector scanning, (b) using a diverging beam, (c) using a diverging beam with weighting by the magnitude-squared coherence function (MSCF), and (d) using a diverging beam with phase coherence factor weighting [19].

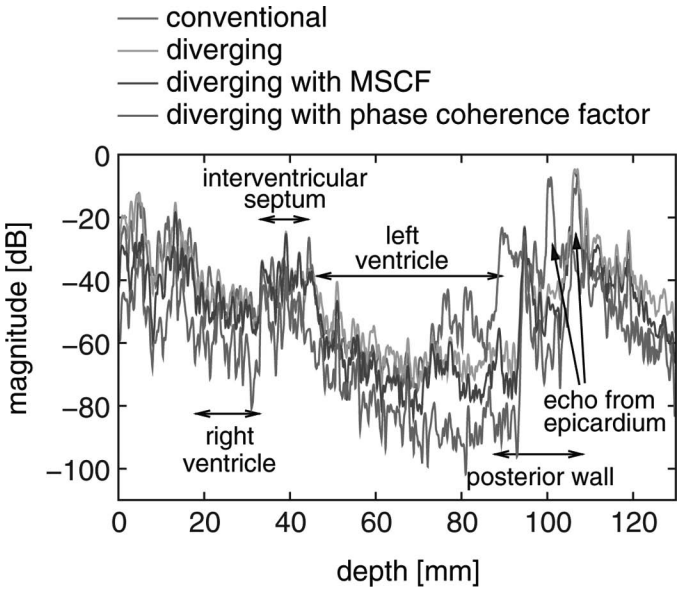

Fig. 5. Intensity profiles along the scan lines indicated by the white lines in Fig. 4.

also well emphasizes specular echoes, such as echoes from heart valves in Fig. 4(d), and relatively strong scattering echoes. The method based on the phase coherence factor and the proposed method are complementary.

In high-frame-rate imaging, it is necessary to use unfocused transmit beams. Therefore, the side lobe level increases in general. Although optimization of transmit conditions, such as angular beam width, angular intervals of transmit beams, estimation of wavefronts of transmit beams, etc., are necessary to further improve the frame rate, such methods for reducing the side lobe level would be necessary for high-frame-rate imaging to obtain an image contrast comparable to or better than that obtained by conventional beamforming.

VI. Conclusions

In this study, a method of suppressing the side lobe level was developed for high-frame-rate echocardiography based on parallel beamforming with diverging transmit beams. To realize suppression of the side lobe level while preserving speckle-like echoes, the MSCF between echoes received by individual transducer elements was used for weighting a beamformed RF echo. Using the proposed method, it was confirmed by basic experiments using fine wires that the side lobe level could be reduced by 4.8 dB compared with conventional beamforming. Furthermore, in *in vivo* measurements, an ultrasonic image of a heart with a full field of view of 90° at a frame rate of 316 Hz could be obtained with an improved image contrast and preservation of speckle-like echoes.

References

[1] H. Kanai, "Propagation of vibration caused by electrical excitation in the normal human heart," *Ultrasound Med. Biol.*, vol. 35, no. 6, pp. 936–948, 2009.

[2] H. Kanai and M. Tanaka, "Minute mechanical-excitation wave-front propagation in human myocardial tissue," *Jpn. J. Appl. Phys.*, vol. 50, no. 7, art. no. 07HA01, 2011.

[3] H. Yoshiara, H. Hasegawa, H. Kanai, and M. Tanaka, "Ultrasonic imaging of propagation of contraction and relaxation in the heart walls at high temporal resolution," *Jpn. J. Appl. Phys.*, vol. 46, no. 7B, pp. 4889–4896, 2007.

[4] H. Kanai, "Propagation of spontaneously actuated pulsive vibration in human heart wall and *in vivo* viscoelasticity estimation," *IEEE Trans. Ultrason. Ferroelectr. Freq. Control*, vol. 52, no. 11, pp. 1931–1942, 2005.

[5] D. M. Bers, *Excitation-Contraction Coupling and Cardiac Contractile Force*, 2nd ed., Dordrecht, The Netherlands: Kluwer Academic, 2001.

[6] E. Konofagou, J. Luo, K. Fujikura, D. Cervantes, and J. Coromilas, "Imaging the electromechanical wave imaging of cardiovascular tissue *in vivo*," in *Proc. IEEE Ultrasonics Symp.*, 2006, pp. 985–988.

[7] E. E. Konofagou, J. D'hooge, and J. Ophir, "Myocardial elastography—A feasibility study *in vivo*," *Ultrasound Med. Biol.*, vol. 28, no. 4, pp. 475–482, 2002.

[8] J. D'hooge, E. Konofagou, F. Jamal, A. Heimdal, L. Barrios, B. Bijnens, J. Thoen, F. van de Werf, G. Sutherland, and P. Suetens, "Two-dimensional ultrasonic strain rate measurement of the human heart *in vivo*," *IEEE Trans. Ultrason. Ferroelectr. Freq. Control*, vol. 49, no. 2, pp. 281–286, 2002.

[9] H. Kanai and Y. Koiwa, "Myocardial rapid velocity distribution," *Ultrasound Med. Biol.*, vol. 27, no. 4, pp. 481–498, 2001.

[10] D. P. Shattuck, M. D. Weinshenker, S. W. Smith, and O. T. v. Ramm, "Explososcan: A parallel processing technique for high speed ultrasound imaging with linear phased arrays," *J. Acoust. Soc. Am.*, vol. 75, no. 4, pp. 1273–1282, 1984.

[11] J. Lu, "2D and 3D high frame rate imaging with limited diffraction beams," *IEEE Trans. Ultrason. Ferroelectr. Freq. Control*, vol. 44, no. 4, pp. 839–856, 1997.

[12] J. Lu, "Experimental study of high frame rate imaging with limited diffraction beams," *IEEE Trans. Ultrason. Ferroelectr. Freq. Control*, vol. 45, no. 1, pp. 84–97, 1998.

[13] J. Cheng and J. Lu, "Extended high-frame rate imaging method with limited-diffraction beams," *IEEE Trans. Ultrason. Ferroelectr. Freq. Control*, vol. 53, no. 5, pp. 880–899, 2006.

[14] J. Lu, J. Cheng, and J. Wang, "High frame rate imaging system for limited diffraction array beam imaging with square-wave aperture weightings," *IEEE Trans. Ultrason. Ferroelectr. Freq. Control*, vol. 53, no. 10, pp. 1796–1812, 2006.

[15] H. Hasegawa and H. Kanai, "High-frame-rate echocardiography using diverging transmit beams and parallel receive beamforming," *J. Med. Ultrasound*, vol. 38, no. 3, pp. 129–140, 2011.

[16] M. O'Donnell and L. J. Thomas, "Efficient synthetic aperture imaging from a circular aperture with possible application to catheter-based imaging," *IEEE Trans. Ultrason. Ferroelectr. Freq. Control*, vol. 39, no. 3, pp. 366–380, 1992.http://www.ncbi.nlm.nih.gov/entrez/query.fcgi?cmd=Retrieve&db=PubMed&list_uids=18267646&dopt=Abstract

[17] M. Karaman and M. O'Donnell, "Synthetic aperture imaging for small scale systems," *IEEE Trans. Ultrason. Ferroelectr. Freq. Control*, vol. 42, no. 3, pp. 429–442, 1995.

[18] F. Gran and J. A. Jensen, "Directional velocity estimation using a spatio-temporal encoding technique based on frequency division for synthetic transmit aperture ultrasound," *IEEE Trans. Ultrason. Ferroelectr. Freq. Control*, vol. 53, no. 7, pp. 1289–1299, 2006.

[19] J. Camacho, M. Parrilla, and C. Fritsch, "Phase coherence imaging," *IEEE Trans. Ultrason. Ferroelectr. Freq. Control*, vol. 56, no. 5, pp. 958–974, 2009.

[20] G. C. Carter, C. H. Knapp, and A. H. Nuttall, "Estimation of the magnitude-squared coherence function via overlapped fast Fourier transform processing," *IEEE Trans. Audio Electroacoust.*, vol. AU-21, no. 4, pp. 337–344, 1983.